

## HIGH-RESOLUTION NONOSCILLATORY CENTRAL SCHEMES FOR HAMILTON–JACOBI EQUATIONS\*

CHI-TIEN LIN<sup>†</sup> AND EITAN TADMOR<sup>‡</sup>

**Abstract.** In this paper, we construct second-order central schemes for multidimensional Hamilton–Jacobi equations and we show that they are nonoscillatory in the sense of satisfying the maximum principle. Thus, these schemes provide the first examples of nonoscillatory second-order Godunov-type schemes based on *global* projection operators. Numerical experiments are performed;  $L^1/L^\infty$ -errors and convergence rates are calculated. For convex Hamiltonians, numerical evidence confirms that our central schemes converge with second-order rates, when measured in the  $L^1$ -norm advocated in our recent paper [*Numer. Math.*, to appear]. The standard  $L^\infty$ -norm, however, fails to detect this second-order rate.

**Key words.** central schemes, Hamilton–Jacobi equations, high resolution, convergence rate

**AMS subject classifications.** Primary, 65M10; Secondary, 35L65

**PII.** S1064827598344856

**1. Introduction.** We consider the numerical solutions by second-order central schemes for the Cauchy problems of the Hamilton–Jacobi (H–J) equation with *Hamiltonian*  $H$ :

$$(1.1) \quad \begin{cases} \partial_t \varphi + H(\nabla_x \varphi) = 0, \\ \varphi(x, 0) = \varphi_0(x). \end{cases}$$

These equations arise mainly from such areas as the calculus of variations, optimal control theory, and differential games. Solutions of H–J equations are continuous and, in the generic case, form discontinuous derivatives in a finite time even with smooth initial conditions. Solutions with this kind of discontinuity are not unique. Therefore, analogous to conservation laws, it is necessary to introduce the concept of the entropy-like condition to facilitate the selection of a unique solution, which leads to the so-called *viscosity solution*. For convex Hamiltonians, the viscosity solution, characterized by a *semiconcave stability* condition, was first introduced by Kruzkov [Kr]. Indeed, such a viscosity solution coincides with the limit solution obtained by the vanishing viscosity method. For general Hamiltonians, the definition of the viscosity solution and the question of well-posedness (in  $L^\infty$ ) were formulated and systematically studied by Crandall, Evans, Lions, Souganidis, and many others [Li, CrLi83, CrEvLi, So]. There is an enormous amount of activity which is based on these studies, and for recent references to the theory viscosity solutions of H–J equations and their applications and for further literature on the subject, we refer the reader to [Ba, BaCr].

We note that H–J equations are closely related to the conservation laws

$$(1.2) \quad \begin{cases} \partial_t u + \sum_{i=1}^n \frac{\partial}{\partial x_i} f_i(u) = 0, \\ u(x, 0) = u_0(x). \end{cases}$$

---

\*Received by the editors September 21, 1998; accepted for publication (in revised form) April 14, 1999; published electronically May 19, 2000. Both authors were partially supported by ONR grant N00014-91-J-1076 and NSF grant DMS97-06827.

<http://www.siam.org/journals/sisc/21-6/34485.html>

<sup>†</sup>Department of Applied Mathematics, Providence University, Shalu 43301, Taiwan (ctlin@pu.edu.tw). Part of this work was done while this author visited the Academia Sinica, Taiwan in December 1997.

<sup>‡</sup>Department of Mathematics, UCLA, Los Angeles, CA, 90095 (tadmor@math.ucla.edu).

Indeed, for one-dimensional H-J equations  $\varphi$  is the viscosity solution of H-J equation (1.1) with Hamiltonian  $H$  if and only if  $u = \frac{\partial}{\partial x}\varphi$  is the entropy solution of conservation laws (1.2) with flux  $f(u) = H(\frac{\partial}{\partial x}\varphi)$  and initial data  $u_0 = \varphi'_0$  [CoFaNa]. In the multidimensional case, however, this kind of one-to-one correspondence no longer exists. Instead,  $\nabla_x\varphi$  satisfies a weakly hyperbolic *system* of conservation laws [Kr, JiXi]. In view of these arguments, we can think of viscosity solutions of the H-J equations (1.1) as primitives of entropy solutions for the conservation laws (1.2). Based on this idea, concepts used for conservation laws can be passed to H-J equations (e.g., [OsSh, LiSo, JiPe, JiXi, HuSh]). In particular, convergence results for approximate solutions of convex conservation laws can be passed to multidimensional convex H-J equations, and in this context we turn to describe our recent work [LinTa].

Turning to the framework of approximate solutions, we let  $\{u^\epsilon\}$  denote an *arbitrary* family of approximate solutions depending on a “small scale”  $\epsilon$ . As examples we mention the vanishing viscosity approximations with viscosity amplitude  $\epsilon$ , e.g., [CrLi83, Kr]; finite difference, finite element, and finite volume solutions based on grid-cells of size  $\epsilon = \Delta x$ , e.g., [Ab, CoFaNa, CrLi84, HuSh, JiPe, JiXi, KoMaSo, KuTa, OsSh, So]; spectral methods depending on  $N = \frac{1}{\epsilon}$  modes, [Le], etc. In [LinTa] we studied the  $L^1$ -convergence of such approximate solutions,  $\varphi^\epsilon$ , for H-J problems with convex Hamiltonians. Our study is a multidimensional extension of the corresponding *Lip'* theory for one-dimensional convex conservation laws developed in [Ta, NeTa92, NeTaTa]. We show that if  $\{\varphi^\epsilon\}$  is stable (in the sense of satisfying the semiconcavity property; consult (3.1) below), then, when measured in the  $L^1$ -norm, one can explicitly estimate the error of such approximate solutions in terms of their truncation and initial errors, namely,

$$\|\varphi(\cdot, t) - \varphi^\epsilon(\cdot, t)\|_{L^1} = C(T) (\|\partial_t\varphi^\epsilon + H(\nabla_x\varphi^\epsilon)\|_{L^1(x,t)} + \|\varphi_0 - \varphi_0^\epsilon\|_{L^1}), \quad 0 \leq t \leq T.$$

When applied to approximate solutions by vanishing viscosity method and Godunov-type schemes, we obtained an order-one error estimate in the  $L^1$ -framework. In this paper, we extend the second-order nonoscillatory (Godunov-type) central schemes developed by Tadmor and his coworkers for nonlinear conservation laws [JiTa, NeTa90] to nonoscillatory central schemes for H-J equations, where we utilize their primitive relation indicated earlier.

The main feature of central schemes for conservation laws is *simplicity* since no (approximate) Riemann solvers and field-by-field decomposition are involved. Based on Godunov-type methods, central schemes consist of successive applications of a discrete projection operator—possibly even a nonlinear projections, followed by the exact evolution operator. This evolution operator is implemented by the finite volume method, which results in a projection operator based on *cell averages*. The Lax–Friedrichs (LxF) scheme is the forerunner of central schemes; it is based on a linear projection—piecewise constant interpolant. The second-order central schemes by Tadmor and his coworkers [NeTa90, JiTa] extend the LxF scheme using nonlinear projection—second- and high-order MUSCL-typed reconstructions [NeTa90, JiTa, LiuTa]. In this paper, we construct central schemes for H-J equations in a similar way. Carrying out the primitive relation indicated earlier, we note that cell averages in conservation laws corresponds to projection operator based on *point-values* in H-J equations.

To construct the first-order central schemes for H-J equations, we start with a point-value linear interpolant. This linear interpolant is then evolved exactly at the center of each cell, which results in a projection based on point-values rather than

cell averages. Our schemes iterates between pointwise projection and evolution. We note that our central schemes are monotone and, hence, they converge in the  $L^\infty$  norm with rate  $\mathcal{O}(\sqrt{\Delta x})$ , with  $\Delta x$  denoting the meshsize [CrLi84]. Moreover, these central schemes were proved by the authors [LinTa] to be first-order in the sense of having  $L^1$ -convergence rate of order  $\mathcal{O}(\Delta x)$ . Again, our central schemes are simple since no (approximate) Riemann solvers are involved. We note in passing that other approaches for the construction of approximate H-J solutions are available.

The second-order central schemes for H-J equations can be constructed in a similar way. Instead of a linear interpolant, we now start with a nonoscillatory *quadratic* interpolant. This quadratic interpolant is then evolved at an interior point of each cell by integrating the H-J equations in time. The time integration is further approximated by the midpoint rule, which results in a two-step scheme. Since our new scheme possesses a similar formula to Jiang and Tadmor's scheme for conservation laws, we are able to prove that this second-order scheme is nonoscillatory in the sense of satisfying the maximum principle, following the lines of [JiTa]. In particular, our schemes provide the first examples of nonoscillatory second-order Godunov-type schemes based on *global* projection operator. Numerical experiments are performed;  $L^1/L^\infty$ -errors and convergence rates are calculated. The error analysis, confirmed by our numerical experiments for convex Hamiltonians, showed a second-order convergence rate of order  $\mathcal{O}(\Delta x)^2$  when measured in the  $L^1$ -norm. This second-order rate is not detected when measured in the  $L^\infty$ -norm, which indicates that the  $L^1$  norm, advocated in [LinTa], is a more appropriate topology as a measure for convergence rate of approximate H-J solutions.

The paper is organized as follows. In section 2, we describe briefly the construction of second-order central schemes for conservation laws in [NeTa90, JiTa]. We then construct central schemes for the one-dimensional H-J equations in section 3.1 and the multidimensional cases in sections 3.2 and 3.3. In section 4, numerical simulations are performed. Errors and convergence rates are calculated in both  $L^1$ - and  $L^\infty$ -frameworks for convex examples.

**2. Central schemes for hyperbolic conservation laws.** Before we construct central schemes for H-J equations, we first detour to a brief review on the construction of second-order central schemes for both one- and multidimensional conservation laws.

*One dimension: The Nessyahu–Tadmor (NT) scheme* [NeTa90]. For one-dimensional conservation laws, the second-order NT scheme is based on reconstructing a piecewise-linear (MUSCL-type) interpolant from the known cell averages at time  $t^n$ ,

$$(2.1) \quad w(x, t^n) = \sum_j \left[ \bar{w}_j^n + w'_j \left( \frac{x - x_j}{\Delta x} \right) \right] \chi_j(x).$$

Here and below,  $w'_j$  denotes the discrete slopes, which results in an overall nonoscillatory scheme. A possible computation of these slopes is given by the family of *discrete derivatives* generalized by the Min-Mod limiter, consult [NeTa90] or see section 3.1 for details. Another more accurate candidate, the UNO limiter, can be found in [HaOs].

This interpolant (2.1) is then evolved exactly in time, projected on the staggered cell-averages at the next time step,  $t^{n+1}$ , and approximated by the midpoint rule, resulting with the two-step *predictor-corrector* form,

$$(2.2) \quad w_j^{n+\frac{1}{2}} = \bar{w}_j^n - \frac{\lambda}{2} f'_j, \quad \lambda = \frac{\Delta t}{\Delta x},$$

$$(2.3) \quad \bar{w}_{j+\frac{1}{2}}^{n+1} = \frac{1}{2}(\bar{w}_j^n + \bar{w}_{j+1}^n) + \frac{1}{8}(w'_j - w'_{j+1}) - \lambda \left[ f(w_{j+1}^{n+1/2}) - f(w_j^{n+1/2}) \right].$$

The values,  $w_j^{n+\frac{1}{2}}$ , given by formula (2.2) are evaluated by Taylor’s expansion. The discrete derivatives of the flux,  $f'_j$ , can be computed, e.g., by  $f'_j = A_j^n w'_j$ , with  $A_j^n := A(\bar{w}_j^n) = f_u(\bar{w}_j^n)$ ; alternatively, one can apply the Min-Mod limiter to each of the components of  $f$ . This componentwise approach is one of the main advantages offered by the central NT schemes over the corresponding characteristic decompositions required by upwind schemes—consult the discussion in [NeTa90], [JiT a].

Before we turn to the multidimensional case, we note that the second-order NT scheme, under the appropriate CFL limitation, satisfies the TVD property and a cell entropy inequality and, hence, converges to the exact entropy solution, at least in the genuinely nonlinear scalar case.

*Multidimensions: The Jiang–Tadmor (JT) scheme* [JiT a]. For simplicity, we illustrate the second-order JT scheme for two-dimensional conservation laws. As in the one-dimensional case, a piecewise-linear (MUSCL-type) interpolant is reconstructed from the calculated cell averages at time  $t^n$ ,  $w(x, y, t^n) = \sum_{j,k} p_{j,k}(x) \chi_{j,k}(x, y)$ , with  $\chi_{j,k}(x, y) := 1_{I_{j,k}}$  denoting the characteristic function over the rectangular mesh  $I_{j,k}$ , where each linear piece,  $p_{j,k}(x, y)$ , over  $I_{j,k}$  is of the form

$$p_{j,k}(x, y) = \bar{w}_{j,k}^n + w'_{j,k} \left( \frac{x - x_j}{\Delta x} \right) + w_{j,k} \left( \frac{y - y_k}{\Delta y} \right).$$

Here and below, the prime and back-prime notations,  $w'_{j,k} \sim \Delta x \partial_x w$ ,  $w_{j,k} \sim \Delta y \partial_y w$ , denote the discrete derivatives in the  $x$ -direction and in the  $y$ -direction, respectively.

This reconstruction is then evolved in time, projected on the staggered cell-averages, and approximated by the midpoint rule to yield the staggered cell-average,  $\bar{w}_{j+\frac{1}{2},k+\frac{1}{2}}^{n+1}$ ,

$$(2.4) \quad \begin{aligned} \bar{w}_{j+\frac{1}{2},k+\frac{1}{2}}^{n+1} &= \frac{1}{4}(\bar{w}_{j,k}^n + \bar{w}_{j+1,k}^n + \bar{w}_{j,k+1}^n + \bar{w}_{j+1,k+1}^n) \\ &+ \frac{1}{16}(w'_{j,k} - w'_{j+1,k} + w'_{j,k+1} - w'_{j+1,k+1}) \\ &+ \frac{1}{16}(w'_{j,k} - w'_{j,k+1} + w'_{j+1,k} - w'_{j+1,k+1}) \\ &- \frac{\lambda}{2} \left[ f(w_{j+1,k}^{n+1/2}) - f(w_{j,k}^{n+1/2}) + f(w_{j+1,k+1}^{n+1/2}) - f(w_{j,k+1}^{n+1/2}) \right] \\ &- \frac{\mu}{2} \left[ g(w_{j,k+1}^{n+1/2}) - g(w_{j,k}^{n+1/2}) + g(w_{j+1,k+1}^{n+1/2}) - g(w_{j+1,k}^{n+1/2}) \right]. \end{aligned}$$

As before, the missing midvalues,  $w^{n+\frac{1}{2}}$ , are evaluated by Taylor’s expansion which results in

$$(2.5) \quad w_{j,k}^{n+\frac{1}{2}} = \bar{w}_{j,k} - \frac{\lambda}{2} f'_{jk} - \frac{\mu}{2} g_{jk}; \quad \lambda = \frac{\Delta t}{\Delta x}, \mu = \frac{\Delta t}{\Delta y}.$$

Before we turn to the construction of central schemes for H-J equations, we note that the JT scheme is nonoscillatory in the sense of satisfying the scalar maximum principle [JiT a, Theorem 3.1].

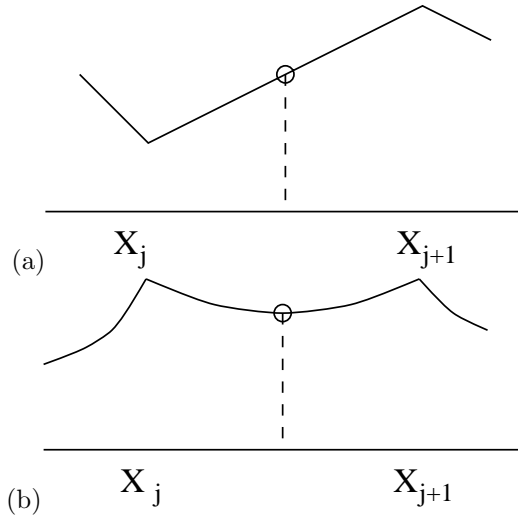


FIG. 3.1. (a) *Linear interpolant for Algorithm 1.* (b) *Quadratic interpolant for Algorithm 2.*

**3. Central schemes for H-J equations.** In the previous section, we used Godunov-type methods to construct central schemes for conservation laws. We evolve in a time step over a controlled volume by the finite volume method, which results in a projection operator based on cell average. Instead, when Godunov-type methods are used for H-J equations, we evolve in a time step and then project on an interior point which results in a *point-value* projection operator. As a main feature, for both conservation laws and H-J equations, our central schemes are simple since no (approximate) Riemann solver is involved. In section 3.1, we construct both first- and second-order central schemes for one-dimensional H-J equations. For the multidimensional cases, we constructed the first-order schemes in section 3.2 and the second-order schemes in section 3.3.

**3.1. The one-dimensional case. First-order.** To construct a first-order central scheme for the one-dimensional H-J equations, we start with a *continuous*, piecewise linear interpolant using the known point values at time  $t^n$ ,  $\varphi(x, t^n) = \varphi_j^n + \frac{\Delta\varphi_j^n}{\Delta x}(x - x_j)$ , where  $x \in I_j := [x_j, x_{j+1}]$  for all  $j$ . This interpolant is then evolved exactly in time and projected at  $(x_{j+\frac{1}{2}}, t^{n+1})$ , resulting in the following formula:

$$\varphi_{j+\frac{1}{2}}^{n+1} = \varphi(x_{j+\frac{1}{2}}, t^n) - \int_{t^n}^{t^{n+1}} H(\partial_x \varphi(x_{j+\frac{1}{2}}, t)) dt.$$

With a CFL restriction,  $\frac{\Delta t}{\Delta x} \max |H'| \leq \frac{1}{2}$ , the integrand is independent of time (at least for a short time step) and, hence, the above formula can be further simplified, leading to the following algorithm.

ALGORITHM 1 (One-dimensional first-order LxF scheme).

$$\varphi_{j+\frac{1}{2}}^{n+1} = \frac{1}{2}(\varphi_j^n + \varphi_{j+1}^n) - \Delta t \cdot H\left(\frac{\Delta\varphi_j^n}{\Delta x}\right).$$

*Second-order.* For a second-order scheme, we start with a continuous piecewise *quadratic* interpolant over each interval  $[x_j, x_{j+1}]$ :

$$\begin{aligned} \varphi(x, t^n) &= \varphi_j^n + \frac{\Delta\varphi_j^n}{\Delta x}(x - x_j) + \frac{\Delta\varphi_j'}{2\Delta x^2}(x - x_j)(x - x_{j+1}) \\ &= \varphi_{j+1}^n \frac{x - x_j}{\Delta x} - \varphi_j^n \frac{x - x_{j+1}}{\Delta x} + \frac{1}{2}\Delta\varphi_j' \left( \frac{x - x_j}{\Delta x} \right) \left( \frac{x - x_{j+1}}{\Delta x} \right), \end{aligned}$$

which is a second-order approximation of  $\varphi$ , (noting that  $\frac{\Delta\varphi_j'}{\Delta x^2} \approx \frac{\partial^2}{\partial x^2} \varphi(x_{j+\frac{1}{2}})$ .) Again,  $\varphi_j'$  is the so-called numerical derivative; for example [NeTa90, JiTa, JLLO1], one can choose any limiter from the following family of *discrete derivatives* parameterized with  $1 \leq \theta \leq 2$ :

$$v_j' = MM(\theta)\{v_{j-1}, v_j, v_{j+1}\} := MM \left( \theta\Delta v_j, \frac{1}{2}(\Delta v_{j-1} + \Delta v_j), \theta\Delta v_{j-1} \right).$$

Here  $MM$  denotes the Min-Mod nonlinear limiter:

$$MM\{x_1, x_2, \dots\} = \begin{cases} \min_j\{x_j\} & \text{if } x_j > 0 \ \forall j, \\ -\min_j\{-x_j\} & \text{if } x_j < 0 \ \forall j, \\ 0 & \text{otherwise.} \end{cases}$$

As in the first-order case, this quadratic interpolant is evolved exactly in time and projected at  $(x_{j+\frac{1}{2}}, t^{n+1})$ , resulting in the following:

$$\varphi_{j+\frac{1}{2}}^{n+1} = \varphi(x_{j+\frac{1}{2}}, t^n) - \int_{t^n}^{t^{n+1}} H(\partial_x \varphi(x_{j+\frac{1}{2}}, t)) dt.$$

With a CFL restriction, the integral on the right-hand side can be evaluated within second-order accuracy by the midpoint rule, yielding

$$\varphi_{j+\frac{1}{2}}^{n+1} = \frac{1}{2}(\varphi_j^n + \varphi_{j+1}^n) - \frac{1}{8}(\varphi_{j+1}' - \varphi_j') - \Delta t \cdot H(\partial_x \varphi(x_{j+\frac{1}{2}}, t^{n+\frac{1}{2}})).$$

Next,  $\partial_x \varphi(x_{j+\frac{1}{2}}, t^{n+\frac{1}{2}})$  can be further approximated by  $\frac{\Delta\varphi_j^{n+\frac{1}{2}}}{\Delta x}$ , and the value  $\varphi_j^{n+\frac{1}{2}}$  can be evaluated by the Taylor expansion, which results in the following algorithm.

ALGORITHM 2 (One-dimensional second-order central scheme).

$$\begin{aligned} \varphi_j^{n+\frac{1}{2}} &= \varphi_j^n - \frac{1}{2}\Delta t \cdot H \left( \frac{\varphi_j'}{\Delta x} \right), \\ \varphi_{j+\frac{1}{2}}^{n+1} &= \frac{1}{2}(\varphi_j^n + \varphi_{j+1}^n) - \frac{1}{8}(\varphi_{j+1}' - \varphi_j') - \Delta t \cdot H \left( \frac{\Delta\varphi_j^{n+\frac{1}{2}}}{\Delta x} \right). \end{aligned}$$

Before we turn to the multidimensional case, we note that our second-order central scheme for H-J equations (1.1) admits a similar form to the NT scheme (2.2), (2.3) constructed in section 2 for one-dimensional conservation laws.

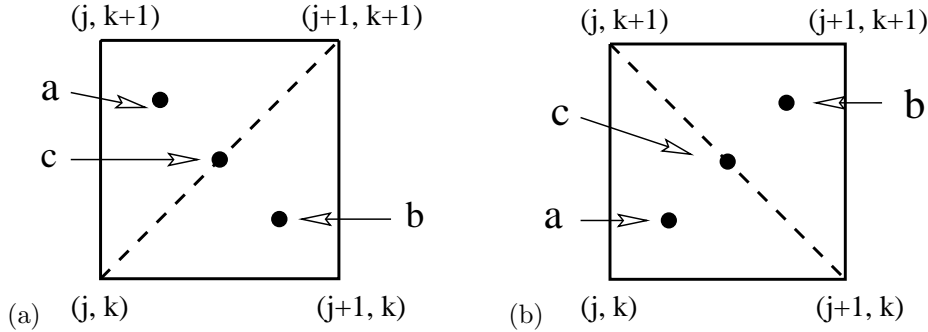


FIG. 3.2. Staggered  $LxF$  schemes for the  $H$ - $J$  equations. (a)  $NW/SE$  division; (b)  $NE/SW$  division.

**3.2. The multidimensional case.** For simplicity, we demonstrate our construction in the two-dimensional case. To approximate the  $H$ - $J$  equation (1.1) by central schemes, we begin with the discrete grid-function,  $\varphi_{jk}^n$ , which represents the point-value at  $x_j := j\Delta x, y_k := k\Delta y$  and  $t = t^n$ . The computational grid consists of cells  $C_{j+\frac{1}{2},k+\frac{1}{2}} := \{(\xi, \eta) \mid |\xi - x_{j+\frac{1}{2}}| \leq \frac{\Delta x}{2}, |\eta - y_{k+\frac{1}{2}}| \leq \frac{\Delta y}{2}\}$  centered around  $(x_{j+\frac{1}{2}}, y_{k+\frac{1}{2}})$ .

*First-order.* We begin with a continuous linear interpolation over each rectangular cell,  $C_{j+\frac{1}{2},k+\frac{1}{2}}$ . Since it is overdetermined, each cell  $C_{j+\frac{1}{2},k+\frac{1}{2}}$  is then divided into two triangles as shown in Figure 3.2 (a) and (b). We shall construct our schemes only based on the mesh divided into  $NW/SE$  triangles shown in Figure 3.2 (a) and denote  $C_{j+\frac{1}{2},k+\frac{1}{2}} = C_{j+\frac{1}{2},k+\frac{1}{2}}^{NW} + C_{j+\frac{1}{2},k+\frac{1}{2}}^{SE}$ . Similar construction applies to the  $NE/SW$  divided mesh in Figure 3.2 (b).

We then construct a continuous linear interpolation over each triangle. On each cell,  $C_{j+\frac{1}{2},k+\frac{1}{2}}$ , the point-value of this interpolant at the interior point,  $\mathbf{a} = (x_{j+\frac{1}{4}}, y_{k+\frac{3}{4}})$  is given by

$$\frac{1}{4} (\varphi_{j,k}^n + 2\varphi_{j,k+1}^n + \varphi_{j+1,k+1}^n)$$

and

$$\frac{1}{4} (\varphi_{j,k}^n + 2\varphi_{j+1,k}^n + \varphi_{j+1,k+1}^n)$$

at the interior point  $\mathbf{b} = (x_{j+\frac{3}{4}}, y_{k+\frac{1}{4}})$ .

With the CFL restriction,  $\Delta t \cdot \max(\frac{1}{\Delta x} |H_u(\nabla\varphi)|, \frac{1}{\Delta y} |H_v(\nabla\varphi)|) \leq \frac{1}{4}$ , we evolve this linear interpolant exactly over a short time period by integrating the  $H$ - $J$  equation (1.1) and project at the next time  $t^{n+1}$ . The value of the point  $\mathbf{a}$  at  $t^{n+1}$  is given by

$$\frac{1}{4} (\varphi_{j,k}^n + 2\varphi_{j,k+1}^n + \varphi_{j+1,k+1}^n) - \Delta t \cdot H \left( \frac{\Delta_x \varphi_{j,k+1}^n}{\Delta x}, \frac{\Delta_y \varphi_{j,k}^n}{\Delta y} \right)$$

and at  $(\mathbf{b}, t^{n+1})$  by

$$\frac{1}{4} (\varphi_{j,k}^n + 2\varphi_{j+1,k}^n + \varphi_{j+1,k+1}^n) - \Delta t \cdot H \left( \frac{\Delta_x \varphi_{j,k}^n}{\Delta x}, \frac{\Delta_y \varphi_{j+1,k}^n}{\Delta y} \right).$$

On each cell,  $C_{j+\frac{1}{2},k+\frac{1}{2}}$ , the new point-value  $\varphi_{j+\frac{1}{2},k+\frac{1}{2}}^{n+1}$  is assigned to be the arithmetic mean of point-values evaluated at  $\mathbf{a}$  and  $\mathbf{b}$ , which results in the following first-order algorithm.

ALGORITHM 3 (Two-dimensional first-order LxF scheme [LinTa]).

$$\begin{aligned} \varphi_{j+\frac{1}{2},k+\frac{1}{2}}^{n+1} &= \frac{1}{4} (\varphi_{j,k}^n + \varphi_{j+1,k}^n + \varphi_{j,k+1}^n + \varphi_{j+1,k+1}^n) \\ &\quad - \frac{\Delta t}{2} \left[ H \left( \frac{\Delta_x \varphi_{j,k}^n}{\Delta x}, \frac{\Delta_y \varphi_{j+1,k}^n}{\Delta y} \right) + H \left( \frac{\Delta_x \varphi_{j,k+1}^n}{\Delta x}, \frac{\Delta_y \varphi_{j,k}^n}{\Delta y} \right) \right]. \end{aligned}$$

Remarks.

- The final scheme for mesh (B) reads

$$\begin{aligned} \varphi_{j+\frac{1}{2},k+\frac{1}{2}}^{n+1} &= \frac{1}{4} (\varphi_{j,k}^n + \varphi_{j+1,k}^n + \varphi_{j,k+1}^n + \varphi_{j+1,k+1}^n) \\ &\quad - \frac{\Delta t}{2} \left[ H \left( \frac{\Delta_x \varphi_{j,k}^n}{\Delta x}, \frac{\Delta_y \varphi_{j,k}^n}{\Delta y} \right) + H \left( \frac{\Delta_x \varphi_{j,k+1}^n}{\Delta x}, \frac{\Delta_y \varphi_{j+1,k}^n}{\Delta y} \right) \right]. \end{aligned}$$

- Our schemes constructed above are staggered in the sense that the computational grid at time  $t^{n+1}$  shifts half a grid-size in each direction. Staggered schemes simplify the interior computation (no upwind) at the expense that they may increase the difficulties of treating the numerical boundary conditions. However, staggered schemes can be converted into nonstaggered ones by using the reaveraging mechanism. Consult [JLLOT, LinTa] for details.

*Remark. On the convergence of the LxF schemes.* In [LinTa], we proved the convergence of the approximate solutions by the family of LxF schemes (Algorithm 3). For completeness, we briefly describe the main ideas here. The reader should consult [LinTa] for details.

For a family of approximate H-J solutions,  $\{\varphi^\epsilon\}$ , which is semiconcave stable, i.e.,  $D^2\varphi^\epsilon(x, t) \leq k(t) \in L^1(0, T)$ , we showed that the  $L^1$ -error can be bounded by the truncation and initial errors; i.e., there holds

$$\|\varphi(\cdot, t) - \varphi^\epsilon(\cdot, t)\|_{L^1} \leq C(T) (\|\partial_t \varphi^\epsilon + H(\nabla_x \varphi^\epsilon)\|_{L^1(x,t)} + \|\varphi_0 - \varphi_0^\epsilon\|_{L^1}), \quad 0 \leq t \leq T.$$

Let  $\varphi^{\Delta x}(x, y, t^n) = \sum \varphi^{\Delta x, NW}(x, y, t^n) \chi_{C^{NW}_{j+\frac{1}{2},k+\frac{1}{2}}} + \varphi^{\Delta x, SE}(x, y, t^n) \chi_{C^{SE}_{j+\frac{1}{2},k+\frac{1}{2}}}$  denote the piecewise linear Godunov-type approximate solution. When applied to Godunov-type schemes, the requirement of semiconcave stability may fail, however, due to the possible “nonconcave” jumps of the piecewise linear approximate solution  $\varphi^\epsilon = \varphi^{\Delta x}(x, y, t^n)$  at the interfaces. To circumvent this difficulty, we introduced the so-called “nearby” approximations,  $\psi^{\Delta x}$ , which are  $\mathcal{O}(\Delta x)$  away from the computed solutions,  $\varphi^{\Delta x}$ . We then apply our  $L^1$ -theory to semiconcave stable “nearby” approximation, resulting in the following theorem.

**THEOREM 3.1** (see [LinTa, Theorem 2.3]). *Let  $\{\varphi^{\Delta x}\}$  be a family of solutions for the Godunov-type scheme, which satisfies the CFL condition  $\Delta t \cdot \max(\frac{1}{\Delta x}|H_u(\nabla\varphi)|, \frac{1}{\Delta y}|H_v(\nabla\varphi)|) \leq \frac{1}{4}$ . Assume the following.*

1. (Consistency)  $\|(I - P_{\Delta x})\varphi^{\Delta x}\|_{L^1} = \mathcal{O}(\Delta x)^2 \|\varphi^{\Delta x}\|_{W^{2,1}}$ , and
2. (Nearby approximations) There exist a family of “nearby” semiconcave stable approximate solutions,  $\{\psi^{\Delta x}(x, t^n)\}$ . Here, “nearby” means that the following holds:

$$\begin{aligned} & \|\partial_t(\varphi^{\Delta x}(\cdot, t) - \psi^{\Delta x}(\cdot, t))\|_{L^1(x)} + \|D_x(\varphi^{\Delta x}(\cdot, t) - \psi^{\Delta x}(\cdot, t))\|_{L^1(x)} \\ & \leq \text{Const} \cdot \Delta x \|\psi^{\Delta x}(\cdot, t)\|_{W^2(L^1(x))}. \end{aligned}$$

Then  $\varphi^{\Delta x}(\cdot, t)$  converges to the exact viscosity solution  $\varphi(\cdot, t)$ , and for any fixed  $T$ , the following estimate holds:

$$\|\varphi^{\Delta x}(\cdot, t) - \varphi(\cdot, t)\|_{L^1(x)} = C_T \Delta x, \quad 0 \leq t \leq T.$$

We note that the semiconcave stable nearby approximation,  $\psi^{\Delta x}$ , can be constructed if the approximate Godunov-type solution,  $\varphi^{\Delta x}$ , satisfies the relaxed *discrete* semiconcave stability: if there exists a  $k(t) \in L^1(0, T)$ ,  $T < \infty$ , such that for all  $h \geq h_0(\epsilon) > 0$  there holds

$$(3.1) \quad D_{h,\xi}^2 \varphi^\epsilon(x, t) := \frac{\varphi^\epsilon(x + h\xi, t) - 2\varphi^\epsilon(x, t) + \varphi^\epsilon(x - h\xi, t)}{h^2} \leq k(t) \quad \forall |\xi| = 1.$$

Indeed, we will demonstrate the construction of such a semiconcave stable nearby approximation in the appendix.

Equipped with these semiconcave stable nearby approximations, we proved the first-order convergence of the LxF schemes, stated in the following theorem.

**THEOREM 3.2** (see [LinTa, Theorem 3.1]). *The approximate solutions,  $\{\varphi^{\Delta x}\}$  by the family of LxF schemes (Algorithm 3) converge to the viscosity solution  $\varphi$ , and the following error estimate holds:*

$$\|\varphi^{\Delta x}(\cdot, t) - \varphi(\cdot, t)\|_{L^1} = \mathcal{O}(\Delta x).$$

**3.3. Second-order central schemes.** In this subsection, we design a second-order central scheme, Algorithm 4, based on Godunov-type methods with a quadratic interpolant over each triangle. This quadratic interpolant is a multidimensional extension of the quadratic interpolant of the second-order central scheme for one-dimensional H-J equations, Algorithm 2 in section 3.1.

For simplicity, we construct our scheme base on the mesh divided into NW/SE triangles shown in Figure 3.2 (a). Similar argument applies to the NE/SW mesh. We first reconstruct a quadratic interpolant over each triangle, which results in

$$\begin{aligned} \varphi^{NW}(x, y) &= \varphi_{j,k} + \frac{\Delta_x \varphi_{j,k+1}}{\Delta x} (x - x_j) + \frac{\Delta_y \varphi_{j,k}}{\Delta y} (y - y_k) \\ &+ \frac{\Delta_x \varphi'_{j,k+1}}{2(\Delta x)^2} (x - x_j)(x - x_{j+1}) + \frac{\Delta_y \varphi'_{j,k} + \Delta_x \varphi'_{j,k+1}}{2\Delta x \Delta y} (x - x_j)(y - y_{k+1}) \\ &+ \frac{\Delta_y \varphi'_{j,k}}{2(\Delta y)^2} (y - y_k)(y - y_{k+1}), \quad (x, y) \in C_{j+\frac{1}{2}, k+\frac{1}{2}}^{NW} \end{aligned}$$

and

$$\begin{aligned} \varphi^{SE}(x, y) &= \varphi_{j,k} + \frac{\Delta_x \varphi_{j,k}}{\Delta x} (x - x_j) + \frac{\Delta_y \varphi_{j+1,k}}{\Delta y} (y - y_k) \\ &+ \frac{\Delta_x \varphi'_{j,k}}{2(\Delta x)^2} (x - x_j)(x - x_{j+1}) + \frac{\Delta_y \varphi'_{j+1,k} + \Delta_x \varphi'_{j,k}}{2\Delta x \Delta y} (x - x_{j+1})(y - y_k) \\ &+ \frac{\Delta_y \varphi'_{j+1,k}}{2(\Delta y)^2} (y - y_k)(y - y_{k+1}), \quad (x, y) \in C_{j+\frac{1}{2}, k+\frac{1}{2}}^{SE}. \end{aligned}$$

We recall that  $\varphi'_{j,k}$  and  $\varphi^{\flat}_{j,k}$  are numerical derivatives. For example, following [NeTa90, JiTa, JLLoT], we can choose

$$\varphi'_{j,k} = MM(\Delta_x \varphi_{j,k}, \Delta_x \varphi_{j-1,k}), \quad \varphi^{\flat}_{j,k} = MM(\Delta_y \varphi_{j,k}, \Delta_y \varphi_{j,k-1}),$$

where  $MM$  denotes the Min-Mod nonlinear limiter. Consult section 3.1 for other possible choices of limiters.

Thus, on each cell,  $C_{j+\frac{1}{2},k+\frac{1}{2}}$ , the point-value of this interpolant at the interior point  $\mathbf{a} = (x_{j+\frac{1}{4}}, y_{k+\frac{3}{4}})$  is given by

$$\begin{aligned} \varphi^{NW}(\mathbf{a}) &:= \frac{1}{4}(\varphi_{j+1,k+1} + 2\varphi_{j,k+1} + \varphi_{j,k}) - \frac{3}{32}(\Delta_x \varphi'_{j,k+1} + \Delta_y \varphi^{\flat}_{j,k}) \\ &\quad - \frac{1}{32}(\Delta_y \varphi'_{j,k} + \Delta_x \varphi^{\flat}_{j,k+1}) \end{aligned}$$

and

$$\begin{aligned} \varphi^{SE}(\mathbf{b}) &:= \frac{1}{4}(\varphi_{j+1,k+1} + 2\varphi_{j+1,k} + \varphi_{j,k}) - \frac{3}{32}(\Delta_x \varphi'_{j,k} + \Delta_y \varphi^{\flat}_{j+1,k}) \\ &\quad - \frac{1}{32}(\Delta_y \varphi'_{j+1,k} + \Delta_x \varphi^{\flat}_{j,k}) \end{aligned}$$

at the interior point  $\mathbf{b} = (x_{j+\frac{3}{4}}, y_{k+\frac{1}{4}})$ .

With the CFL restriction,  $\Delta t \cdot \max(\frac{1}{\Delta x} |H_u(\nabla \varphi)|, \frac{1}{\Delta y} |H_v(\nabla \varphi)|) \leq \frac{1}{4}$ , we evolve this quadratic interpolant exactly over a short time period by integrating the H-J equation (1.1) and projecting it at the time  $t^{n+1}$ . The value of the point  $\mathbf{a}$  at  $t^{n+1}$  is given by

$$\varphi^{NW}(\mathbf{a}) - \Delta t \cdot H \left( \frac{\Delta_x \varphi_{j,k+1}^{n+\frac{1}{2}}}{\Delta x}, \frac{\Delta_y \varphi_{j,k}^{n+\frac{1}{2}}}{\Delta y} \right)$$

and at  $(\mathbf{b}, t^{n+1})$  by

$$\varphi^{SE}(\mathbf{b}) - \Delta t \cdot H \left( \frac{\Delta_x \varphi_{j,k}^{n+\frac{1}{2}}}{\Delta x}, \frac{\Delta_y \varphi_{j+1,k}^{n+\frac{1}{2}}}{\Delta y} \right).$$

The average of the last two point values is only of first-order accurate approximation to the midcell value; to obtain a second-order scheme, we construct a quadratic interpolant on the segment connecting points  $\mathbf{a}$  and  $\mathbf{b}$  based on the point-values  $\varphi(\mathbf{a})$  and  $\varphi(\mathbf{b})$ , i.e.,

$$\varphi^{n+1}(\mathbf{b})(\mathbf{x} - \mathbf{a}) \cdot \mathbf{n} - \varphi^{n+1}(\mathbf{a})(\mathbf{x} - \mathbf{b}) \cdot \mathbf{n} + \frac{1}{2} S \cdot ((\mathbf{x} - \mathbf{a}) \cdot \mathbf{n}) \cdot ((\mathbf{x} - \mathbf{b}) \cdot \mathbf{n}),$$

where  $\mathbf{n} = \frac{\mathbf{b}-\mathbf{a}}{|\mathbf{b}-\mathbf{a}|}$  and  $S$  is the second-order total differential of  $\varphi$  along  $\mathbf{n}$  at the point  $\mathbf{c} := \frac{1}{2}(\mathbf{a} + \mathbf{b}) = (x_{j+\frac{1}{2}}, y_{k+\frac{1}{2}})$ . Since  $S$  can be approximated using the data at the time  $t^n$  level, we take

$$\begin{aligned} S &= \frac{1}{4}(\varphi'_{i+1,k} - \varphi'_{i,k+1} + \varphi^{\flat}_{i,k+1} - \varphi^{\flat}_{i+1,k}) \\ &\simeq \frac{\partial^2}{\partial x^2} \varphi(\mathbf{c}) \left( \frac{\Delta x}{2} \right)^2 - 2 \frac{\partial^2}{\partial x \partial y} \varphi(\mathbf{c}) \frac{\Delta x \Delta y}{4} + \frac{\partial^2}{\partial y^2} \varphi(\mathbf{c}) \left( \frac{\Delta y}{2} \right)^2 + \mathcal{O}(\Delta x)^3. \end{aligned}$$

The point value  $\varphi_{j+\frac{1}{2},k+\frac{1}{2}}^{n+1}$  is then given by this quadratic interpolant evaluated at the center point  $\mathbf{c}$ , which results in the following second-order scheme.

ALGORITHM 4 (Two-dimensional second-order central scheme).

$$\begin{aligned} \varphi_{j+\frac{1}{2},k+\frac{1}{2}}^{n+1} &= \frac{1}{4}(\varphi_{j,k}^n + \varphi_{j+1,k}^n + \varphi_{j,k+1}^n + \varphi_{j+1,k+1}^n) \\ &\quad + \frac{1}{16}(\varphi'_{j,k} - \varphi'_{j+1,k} + \varphi'_{j,k+1} - \varphi'_{j+1,k+1}) \\ &\quad + \frac{1}{16}(\varphi^{\flat}_{j,k} - \varphi^{\flat}_{j,k+1} + \varphi^{\flat}_{j+1,k} - \varphi^{\flat}_{j+1,k+1}) \\ &\quad - \frac{\Delta t}{2} \left[ H \left( \frac{\Delta_x \varphi_{j,k}^{n+\frac{1}{2}}}{\Delta x}, \frac{\Delta_y \varphi_{j+1,k}^{n+\frac{1}{2}}}{\Delta y} \right) + H \left( \frac{\Delta_x \varphi_{j,k+1}^{n+\frac{1}{2}}}{\Delta x}, \frac{\Delta_y \varphi_{j,k}^{n+\frac{1}{2}}}{\Delta y} \right) \right], \end{aligned}$$

where

$$(3.2) \quad \varphi_{j,k}^{n+\frac{1}{2}} := \varphi_{j,k} - \frac{\Delta t}{2} H \left( \frac{\varphi'_{j,k}}{\Delta x}, \frac{\varphi^{\flat}_{j,k}}{\Delta y} \right).$$

Our second-order central scheme, Algorithm 4, is a high-order extension of the first-order staggered LxF scheme, Algorithm 3. We also note that our new scheme, Algorithm 4, admits a formula analogous to the two-dimensional JT scheme (2.4). Indeed, following the lines of the proof for the JT scheme, we obtain the following theorem.

THEOREM 3.3. *Algorithm 4 is nonoscillatory in the sense of satisfying the maximum principle. Namely, there exists a sufficiently small CFL number,  $C_\theta$  (e.g.,  $C_1 = (\sqrt{7} - 2)/6 \sim 0.1$ ), such that if the CFL condition is fulfilled,*

$$\max \left( \frac{\Delta t}{\Delta x} \cdot \max_{u,v} |H_u(u,v)|, \frac{\Delta t}{\Delta y} \cdot \max_{u,v} |H_v(u,v)| \right) \leq C_\theta,$$

then the following local maximum principle holds:

$$(3.3) \quad \min_{\substack{|p-(j+\frac{1}{2})|=\frac{1}{2} \\ |q-(k+\frac{1}{2})|=\frac{1}{2}}} \{\varphi_{p,q}^n\} \leq \varphi_{j+\frac{1}{2},k+\frac{1}{2}}^{n+1} \leq \max_{\substack{|p-(j+\frac{1}{2})|=\frac{1}{2} \\ |q-(k+\frac{1}{2})|=\frac{1}{2}}} \{\varphi_{p,q}^n\}.$$

*Proof.* Without loss of generality, we assume  $H(0,0) = 0$ . By taking a Taylor expansion on those Hamiltonian terms, we can rewrite the new value computed in Algorithm 4,  $\varphi_{j+\frac{1}{2},k+\frac{1}{2}}^{n+1}$ , as the average of four distinctive terms

$$\begin{aligned} \varphi_{j+\frac{1}{2},k+\frac{1}{2}}^{n+1} &= \frac{1}{4} \times \left\{ \frac{1}{2} (\varphi_{j,k}^n + \varphi_{j+1,k}^n) + \frac{1}{4} (\varphi'_{j,k} - \varphi'_{j+1,k}) - 2\lambda H_u(\bullet) \Delta_x \varphi_{j,k}^{n+\frac{1}{2}} \right. \\ &\quad + \frac{1}{2} (\varphi_{j,k+1}^n + \varphi_{j+1,k+1}^n) + \frac{1}{4} (\varphi'_{j,k+1} - \varphi'_{j+1,k+1}) - 2\mu H_v(\bullet) \Delta_y \varphi_{j+1,k}^{n+\frac{1}{2}} \\ (3.4) \quad &\quad + \frac{1}{2} (\varphi_{j,k}^n + \varphi_{j,k+1}^n) + \frac{1}{4} (\varphi^{\flat}_{j,k} - \varphi^{\flat}_{j,k+1}) - 2\lambda H_u(\bullet) \Delta_x \varphi_{j,k+1}^{n+\frac{1}{2}} \\ &\quad \left. + \frac{1}{2} (\varphi_{j+1,k}^n + \varphi_{j+1,k+1}^n) + \frac{1}{4} (\varphi^{\flat}_{j+1,k} - \varphi^{\flat}_{j+1,k+1}) - 2\mu H_v(\bullet) \Delta_y \varphi_{j,k}^{n+\frac{1}{2}} \right\} \\ &=: \frac{1}{4} \times \{\mathcal{I}_1 + \mathcal{I}_2 + \mathcal{I}_3 + \mathcal{I}_4\}. \end{aligned}$$

Here  $\lambda := \frac{\Delta t}{\Delta x}$ ,  $\mu := \frac{\Delta t}{\Delta y}$ .  $H_u(\bullet)$  and  $H_v(\bullet)$  are of some unspecified intermediate values. We will show that each of these four terms,  $\mathcal{I}_j$ , can be written as an appropriate sum

of the point values at  $t^n$ ,  $\{\varphi_{jk}^n, \varphi_{j+1,k}^n, \varphi_{j,k+1}^n, \varphi_{j+1,k+1}^n\}$ , so that  $\varphi_{j+\frac{1}{2},k+\frac{1}{2}}^{n+\frac{1}{2}}$  can be expressed as a *convex* combination of these averages. This implies, in particular, that the local maximum principle (3.3) holds.

We begin by estimating the difference between two neighboring midvalues,  $\Delta_x \varphi_{jk}^{n+\frac{1}{2}} := \varphi_{j+1,k}^{n+\frac{1}{2}} - \varphi_{jk}^{n+\frac{1}{2}}$ , evaluated in the predictor step (3.2), with the help of a Taylor expansion on  $H(u, v)$ ,

$$\begin{aligned} \varphi_{j+1,k}^{n+\frac{1}{2}} - \varphi_{jk}^{n+\frac{1}{2}} &= \varphi_{j+1,k} - \varphi_{jk} + \frac{\Delta t}{2} \left[ H \left( \frac{\varphi'_{j+1,k}}{\Delta x}, \frac{\varphi'_{j+1,k}}{\Delta y} \right) - H \left( \frac{\varphi'_{j,k}}{\Delta x}, \frac{\varphi'_{j,k}}{\Delta y} \right) \right] \\ (3.5) \qquad &= \varphi_{j+1,k} - \varphi_{jk} + \frac{\lambda}{2} H_u(\bullet) \Delta_x \varphi'_{j,k} + \frac{\mu}{2} H_v(\bullet) \Delta_x \varphi'_{j,k}. \end{aligned}$$

Since  $\varphi'_{j+1,k}$  and  $\varphi'_{j,k}$  cannot have opposite signs, thanks to Min-Mod limiters, their differences on the right of (3.5) does not exceed

$$(3.6) \qquad |\varphi'_{j+1,k} - \varphi'_{j,k}| \leq |\varphi_{j+1,k}^n - \varphi_{jk}^n|.$$

The third difference on the right of (3.5),  $\Delta_x \varphi_{j,k}^\lambda := \varphi_{j+1,k}^\lambda - \varphi_{jk}^\lambda$ , represents a ‘‘mixed’’ derivative (which allows for opposite signs); here we use the definition of the Min-Mod limiter, resulting in

$$(3.7) \qquad \begin{aligned} |\varphi_{j+1,k}^\lambda - \varphi_{jk}^\lambda| &\leq |\varphi_{j+1,k}^\lambda| + |\varphi_{jk}^\lambda| \\ &\leq |\varphi_{j+1,k+1}^n - \varphi_{j+1,k}^n| + |\varphi_{j,k+1}^n - \varphi_{jk}^n|. \end{aligned}$$

Using (3.6) and (3.7) we obtain an upper bound on the midvalues difference in (3.5), which, in turn, enables us to upper bound the corresponding ‘‘flux’’ difference

$$\begin{aligned} \lambda |H_u(\bullet) \Delta_x \varphi_{jk}^{n+\frac{1}{2}}| &\leq \lambda \mathbf{a} |\varphi_{j+1,k}^{n+\frac{1}{2}} - \varphi_{jk}^{n+\frac{1}{2}}| \\ &\leq \frac{1}{2} \lambda \mathbf{a} (2 + \lambda \mathbf{a}) |\varphi_{j+1,k}^n - \varphi_{jk}^n| \\ (3.8) \qquad &+ \frac{1}{2} \lambda \mathbf{a} \cdot \mu \mathbf{b} [|\varphi_{j,k+1}^n - \varphi_{jk}^n| + |\varphi_{j+1,k+1}^n - \varphi_{j+1,k}^n|]. \end{aligned}$$

Here and below,  $\mathbf{a} := \max_{u,v} |H_u(u, v)|$  and  $\mathbf{b} := \max_{u,v} |H_v(u, v)|$  denote the maximal speeds in the  $x$ - and  $y$ -directions.

We now return to the first term,  $\mathcal{I}_1$ , in (3.4): by (3.8), it does not exceed

$$\begin{aligned} \mathcal{I}_1 &\leq \frac{1}{2} (\varphi_{jk}^n + \varphi_{j+1,k}^n) + \left( \frac{1}{4} + \lambda \mathbf{a} (2 + \lambda \mathbf{a}) \right) |\varphi_{j+1,k}^n - \varphi_{jk}^n| \\ &\quad + \lambda \mathbf{a} \cdot \mu \mathbf{b} |\varphi_{j,k+1}^n - \varphi_{jk}^n| + \lambda \mathbf{a} \cdot \mu \mathbf{b} |\varphi_{j+1,k+1}^n - \varphi_{j+1,k}^n|. \end{aligned}$$

Thus

$$(3.9) \qquad \mathcal{I}_1 \leq \mathcal{I}_{11} + \mathcal{I}_{12} + \mathcal{I}_{13} + \mathcal{I}_{14},$$

where

$$\begin{aligned} \mathcal{I}_{11} &= \frac{1}{2} (\varphi_{jk}^n + \varphi_{j+1,k}^n), \quad \mathcal{I}_{12} = \alpha |\varphi_{j+1,k}^n - \varphi_{jk}^n|, \quad \alpha := \frac{1}{4} + \lambda \mathbf{a} (2 + \lambda \mathbf{a}), \\ \mathcal{I}_{13} &= \beta |\varphi_{j,k+1}^n - \varphi_{jk}^n|, \quad \mathcal{I}_{14} = \beta |\varphi_{j+1,k+1}^n - \varphi_{j+1,k}^n|, \quad \beta := \lambda \mathbf{a} \cdot \mu \mathbf{b}. \end{aligned}$$

In a similar manner we obtain

$$(3.10) \quad \mathcal{I}_2 \leq \frac{1}{2}(\varphi_{j,k+1}^n + \varphi_{j+1,k+1}^n) + \alpha|\varphi_{j+1,k+1}^n - \varphi_{j,k+1}^n| \\ + \beta|\varphi_{j,k+1}^n - \varphi_{jk}^n| + \beta|\varphi_{j+1,k+1}^n - \varphi_{j+1,k}^n| =: \mathcal{I}_{21} + \mathcal{I}_{22} + \mathcal{I}_{23} + \mathcal{I}_{24},$$

$$(3.11) \quad \mathcal{I}_3 \leq \frac{1}{2}(\varphi_{jk}^n + \varphi_{j,k+1}^n) + \alpha|\varphi_{j,k+1}^n - \varphi_{jk}^n| \\ + \beta|\varphi_{j+1,k}^n - \varphi_{jk}^n| + \beta|\varphi_{j+1,k+1}^n - \varphi_{j,k+1}^n| =: \mathcal{I}_{31} + \mathcal{I}_{32} + \mathcal{I}_{33} + \mathcal{I}_{34},$$

and finally

$$(3.12) \quad \mathcal{I}_4 \leq \frac{1}{2}(\varphi_{j+1,k}^n + \varphi_{j+1,k+1}^n) + \alpha|\varphi_{j+1,k+1}^n - \varphi_{j+1,k}^n| \\ + \beta|\varphi_{j+1,k}^n - \varphi_{j,k}^n| + \beta|\varphi_{j+1,k+1}^n - \varphi_{j,k+1}^n| =: \mathcal{I}_{41} + \mathcal{I}_{42} + \mathcal{I}_{43} + \mathcal{I}_{44}.$$

We now conclude by regrouping similar terms in the last four bounds; specifically, we rearrange the summation of the last four bounds in (3.9)–(3.12),

$$\sum_{j=1}^4 \mathcal{I}_j = (\mathcal{I}_{11} + \mathcal{I}_{12} + \mathcal{I}_{33} + \mathcal{I}_{43}) + (\mathcal{I}_{21} + \mathcal{I}_{22} + \mathcal{I}_{34} + \mathcal{I}_{44}) + \cdots,$$

and we obtain

$$\varphi_{j+\frac{1}{2},k+\frac{1}{2}}^{n+1} = \frac{1}{4} \sum_{j=1}^4 \mathcal{I}_j \\ \leq \frac{1}{4} \times \left\{ \frac{1}{2}(\varphi_{jk}^n + \varphi_{j+1,k}^n) + (\alpha + 2\beta)|\varphi_{j+1,k}^n - \varphi_{jk}^n| \right. \\ + \frac{1}{2}(\varphi_{j,k+1}^n + \varphi_{j+1,k+1}^n) + (\alpha + 2\beta)|\varphi_{j+1,k+1}^n - \varphi_{j,k+1}^n| \\ + \frac{1}{2}(\varphi_{jk}^n + \varphi_{j,k+1}^n) + (\alpha + 2\beta)|\varphi_{j,k+1}^n - \varphi_{jk}^n| \\ \left. + \frac{1}{2}(\varphi_{j+1,k}^n + \varphi_{j+1,k+1}^n) + (\alpha + 2\beta)|\varphi_{j+1,k+1}^n - \varphi_{j+1,k}^n| \right\}.$$

Our assertion concerning the convex combination, and hence the local maximum principle follows, provided the following inequalities hold:

$$(3.13) \quad \alpha + 2\beta \equiv \frac{1}{4} + \lambda \mathbf{a} (2 + \lambda \mathbf{a} + 2\mu \mathbf{b}) \leq \frac{1}{2},$$

$$(3.14) \quad \alpha + 2\beta \equiv \frac{1}{4} + \mu \mathbf{b} (2 + \mu \mathbf{b} + 2\lambda \mathbf{a}) \leq \frac{1}{2}.$$

Clearly, these inequalities are satisfied for a sufficiently small CFL number. For example, (3.13)–(3.14) hold provided  $\max(\lambda \mathbf{a}, \mu \mathbf{b})$  does not exceed the largest root of  $12\kappa^2 + 8\kappa - 1 = 0$ , which yields (3.3).  $\square$

*Remark.* Our proof holds for generalized Min-Mod limiters,  $MM(\theta)$  with  $1 \leq \theta \leq 2$ , stated in section 3.1. In that case,  $\alpha$  and  $\beta$  are replaced by  $\frac{\theta}{4} + \lambda \mathbf{a}(2 + \theta \cdot \lambda \mathbf{a})$  and  $\theta \cdot \lambda \mathbf{a} \cdot \mu \mathbf{b}$ , respectively.

*Remark.* If the Hamiltonian also depends on spatial variables, the second-order scheme then reads as in the following algorithm.

ALGORITHM 5 (Two-dimensional second-order central scheme, variable coefficient).

$$\begin{aligned} \varphi_{j+\frac{1}{2},k+\frac{1}{2}}^{n+1} &= \frac{1}{4}(\varphi_{j,k}^n + \varphi_{j+1,k}^n + \varphi_{j,k+1}^n + \varphi_{j+1,k+1}^n) \\ &+ \frac{1}{16}(\varphi'_{j,k} - \varphi'_{j+1,k} + \varphi'_{j,k+1} - \varphi'_{j+1,k+1}) \\ &+ \frac{1}{16}(\varphi^{\backslash}_{j,k} - \varphi^{\backslash}_{j,k+1} + \varphi^{\backslash}_{j+1,k} - \varphi^{\backslash}_{j+1,k+1}) \\ &- \frac{\Delta t}{2} \left[ H \left( x_{j+\frac{1}{2}}, y_{j+\frac{1}{2}}, \frac{\Delta_x \varphi_{j,k}^{n+\frac{1}{2}}}{\Delta x}, \frac{\Delta_y \varphi_{j+1,k}^{n+\frac{1}{2}}}{\Delta y} \right) \right. \\ &\left. + H \left( x_{j+\frac{1}{2}}, y_{j+\frac{1}{2}}, \frac{\Delta_x \varphi_{j,k+1}^{n+\frac{1}{2}}}{\Delta x}, \frac{\Delta_y \varphi_{j,k}^{n+\frac{1}{2}}}{\Delta y} \right) \right], \end{aligned}$$

where  $\varphi'_{j,k}$ ,  $\varphi^{\backslash}_{j,k}$  and  $\varphi_{j,k}^{n+\frac{1}{2}}$  are defined as above.

*Remark.* On the convergence of the second-order schemes. The question of convergence in the second-order case, and in particular the issue of convergence rate, is more intricate than in the previous first-order setup. A key open problem in this context is the question of semiconcave stability. Assume that our second-order central (Godunov-type) scheme satisfies the discrete semiconcave stability (3.1). Then, there exists an admissible family of nearby “approximate” solutions,  $\psi^{\Delta x}$ , constructed in the appendix, and hence Theorem 3.1 holds. Namely, we find

$$\|\varphi^{\Delta x}(\cdot, t) - \varphi(\cdot, t)\|_{L^1} = \mathcal{O}(\Delta x).$$

Though the last error estimate is restricted to first-order rate, numerical evidence confirms a second-order convergence rate,  $\|\varphi^{\Delta x}(\cdot, t) - \varphi(\cdot, t)\|_{L^1} = \mathcal{O}(\Delta x)^2$ , which follows from the second-order consistency  $\|(I - P_{\Delta x})\varphi^{\Delta x}\|_{L^1} = \mathcal{O}(\Delta x)^3 \|\varphi^{\Delta x}\|_{W^{2,1}}$ . A proof for such second-order consistency for  $W^{2,1}$ -solutions is open. We note that such a second-order consistency estimate, however, is expected for the class of *piecewise smooth* solutions [TaTa]. Indeed, in practice, one encounters only the subclass of  $W^{2,1}$  piecewise solutions.

**4. Numerical experiments for H-J equations.** In this section, we implement our schemes constructed in section 3 for both one- and multidimensional H-J equations.  $L^1$ - and  $L^\infty$ -errors, and convergence rates are calculated and compared in subsection 4.1. Several examples solved by the second-order schemes are presented in subsection 4.2.

**4.1. Convergence rate tests.** *Example 1* (one dimension). We first solve the one-dimensional periodic H-J equations:

$$(4.1) \quad \begin{cases} \varphi_t + H(\varphi_x) = 0, & -1 \leq x \leq 1 \\ \varphi(x, 0) = -\cos(\pi x), \end{cases}$$

with a strictly convex Hamiltonian  $H$  (Burgers-type equation)

$$H(u) = \frac{(u + \alpha)^2}{2}$$

TABLE 1  
*Errors and orders for Example 1 via Algorithm 1, first-order.*

N	Time = 0.5/π <sup>2</sup>				Time = 1.5/π <sup>2</sup>			
	L <sup>1</sup>		L <sup>∞</sup>		L <sup>1</sup>		L <sup>∞</sup>	
	Error	Order	Error	Order	Error	Order	Error	Order
Convex Hamiltonian								
20	0.0773	-	0.0885	-	0.1320	-	0.1011	-
40	0.0309	1.32	0.0387	1.20	0.0668	0.98	0.0820	0.30
80	0.0155	1.00	0.0203	0.93	0.0325	1.04	0.0355	1.21
160	0.0072	1.10	0.0097	1.07	0.0161	1.02	0.0144	1.30
320	0.0036	1.00	0.0049	0.98	0.0080	1.01	0.0065	1.16
640	0.0018	1.03	0.0024	1.02	0.0040	1.00	0.0032	1.00
1280	0.0009	1.00	0.0012	0.99	0.0020	1.00	0.0019	0.77
Nonconvex Hamiltonian								
20	0.0248	-	0.0281	-	0.0390	-	0.0618	-
40	0.0123	1.01	0.0153	0.87	0.0189	1.05	0.0342	0.85
80	0.0042	1.55	0.0058	1.40	0.0069	1.44	0.0125	1.45
160	0.0015	1.45	0.0024	1.26	0.0033	1.06	0.0062	1.01
320	0.0008	1.00	0.0013	0.96	0.0017	1.01	0.0057	0.12
640	0.0004	1.12	0.0006	1.08	0.0008	1.08	0.0028	1.02
1280	0.0002	1.06	0.0003	1.04	0.0004	1.04	0.0013	1.09

and a nonconvex Hamiltonian  $H$ :

$$H(u) = -\cos(u + \alpha).$$

The exact solution can be found through the solution of the corresponding conservation laws after changing variables—consult Shu and Osher [OsSh] for details. For simplicity, we take  $\alpha = 1$ . For the convex case, the singularity occurs at time  $t = 1/\pi^2$ , and near this time for the nonconvex case. We calculate the order of the error under the discrete  $l^1$  norm

$$\|e(\cdot, T)\|_{l^1} := \Delta x \sum_i |e(x_i, T)|.$$

Both the first-order scheme, Algorithm 1, and the second-order scheme, Algorithm 2, are used for this example. We recorded data at  $t_1 = 0.5/\pi^2$  (before singularity) and  $t_2 = 1.5/\pi^2$  (after singularity).  $L^1$ - and  $L^\infty$ -errors and convergence rates are calculated and listed in Tables 1 and 2 for Algorithms 1 and 2, respectively. The resolution of numerical solutions are also presented in Figure 4.1.

For both convex and nonconvex Hamiltonians, the results quoted in Table 1 show an  $L^1$ -convergence rate of order  $\mathcal{O}(\Delta x)$  for both before and after the formation of the singularity. At the same time, Table 1 also records the same order of  $L^\infty$ -convergence even after the formation of the singularity. The discrepancy between the optimal  $L^\infty$ -result of order  $\mathcal{O}(\sqrt{\Delta x})$  [CrLi84, So] and the result of Table 1 is similar to the discrepancy in the  $L^1$ -error for convex conservation laws. Although the optimal result for conservation laws is of order  $\mathcal{O}(\sqrt{\Delta x})$ , still, when computing with finitely many shock discontinuities, we find a convergence rate of order  $\mathcal{O}(\Delta x)$  [TaTe, TaTa]. In particular, since all we can compute are solutions with finitely many singularities, we cannot distinguish between the convergence rates of first-order H-J solutions when measured either by  $L^1$ - or  $L^\infty$ -norm—they both are of order  $\mathcal{O}(\Delta x)$ .

Table 2 quotes the results for the second-order central scheme, Algorithm 2, for both convex and nonconvex cases. Here the  $L^1$ -measure of the error achieves the

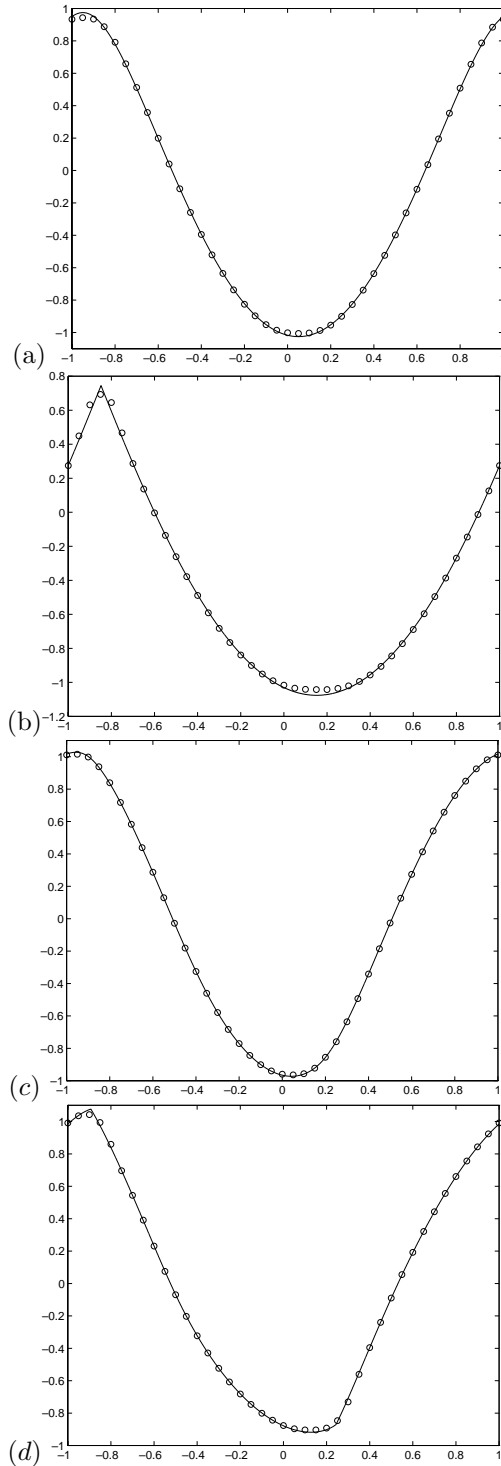


FIG. 4.1. Resolution for Example 1 via Algorithm 2, second-order. Mesh: 40. (a) and (b), for the convex Hamiltonian; (c) and (d), for the nonconvex Hamiltonian. (a) and (c), before singularity,  $t = 0.5/\pi^2$ ; (b) and (d), after singularity,  $t = 1.5/\pi^2$ .

TABLE 2  
*Errors and orders for Example 1 via Algorithm 2, second-order.*

N	Time = 0.5/π <sup>2</sup>				Time = 1.5/π <sup>2</sup>			
	L <sup>1</sup>		L <sup>∞</sup>		L <sup>1</sup>		L <sup>∞</sup>	
	Error	Order	Error	Order	Error	Order	Error	Order
Convex Hamiltonian								
20	0.04233	-	0.0611	-	0.06333	-	0.0919	-
40	0.01144	1.88	0.0307	0.99	0.02305	1.46	0.0512	0.84
80	0.00295	1.96	0.0123	1.32	0.00607	1.93	0.0263	0.96
160	0.00079	1.90	0.0051	1.26	0.00165	1.88	0.0129	1.03
320	0.00021	1.90	0.0021	1.28	0.00039	2.10	0.0061	1.09
640	0.00006	1.94	0.0008	1.31	0.00010	1.94	0.0033	0.88
1280	0.00001	1.95	0.0003	1.32	0.00003	1.97	0.0015	1.13
Nonconvex Hamiltonian								
20	0.017701	-	0.02601	-	0.03615	-	0.0790	-
40	0.003669	2.27	0.01123	1.21	0.00935	1.95	0.0312	1.34
80	0.000804	2.19	0.00379	1.57	0.00223	2.07	0.0104	1.58
160	0.000186	2.11	0.00140	1.44	0.00055	2.01	0.0061	0.78
320	0.000046	2.03	0.00058	1.26	0.00015	1.85	0.0037	0.70
640	0.000011	1.99	0.00023	1.35	0.00004	1.91	0.0016	1.18
1280	0.000003	1.96	0.00009	1.27	0.00001	2.08	0.0006	1.36

expected convergence rate of order  $\mathcal{O}(\Delta x)^2$  both before and after singularities occur, in contrast to a lower rate of convergence when measured in the  $L^\infty$ -norm.

Our numerical evidence supports the  $L^1$ -error estimates for the approximate solutions of *convex* H-J equations in the previous paper [LinTà]: The  $L^1$ -norm is an appropriate measure for convergence rate problems of approximate solutions to *convex* H-J equations.

*Example 2* (two dimensions). We solve the two-dimensional periodic H-J equations

$$(4.2) \quad \begin{cases} \varphi_t + H(\varphi_x, \varphi_y) = 0, \\ \varphi(x, y, 0) = -\cos(\pi \frac{x+y}{2}), \end{cases} \quad -2 \leq x, y \leq 2,$$

with a strictly convex Hamiltonian  $H$  (Burgers-type equation)

$$H(u, v) = \frac{(u + v + 1)^2}{2}$$

and a nonconvex Hamiltonian  $H$

$$H(u, v) = -\cos(u + v + 1).$$

Under the transformation,  $\xi = \frac{1}{2}(x + y)$  and  $\eta = \frac{1}{2}(x - y)$ , our test problem (4.2) becomes the one-dimensional problem in the  $\xi$  direction, (4.1) in Example 1. The exact solution, therefore, can be found through the solution of the corresponding one-dimensional conservation laws [OsSh]. We note that since we program in the  $(x, y)$ -coordinate system, this is a genuine two-dimensional problem.

As in the Example 1, the singularity occurs at time  $t = 1/\pi^2$  for the convex Hamiltonian and near this time for the nonconvex case. The first-order scheme, staggered LxF schemes, Algorithm 3, referred as  $LxF$ , and the second-order scheme, Algorithm 4, are used in this example. We calculate the order of the error under the discrete  $l^1$ -norm

$$\|e(\cdot, \cdot, T)\|_{l^1} := \Delta x \Delta y \sum_{i,j} |e(x_i, y_j, T)|.$$

TABLE 3  
*Errors and orders for Example 4 via Algorithm 3, first-order.*

N	Time = $0.5/\pi^2$				Time = $1.5/\pi^2$			
	$L^1$		$L^\infty$		$L^1$		$L^\infty$	
	Error	Order	Error	Order	Error	Order	Error	Order
20	1.2814	-	0.1651	-	1.9204	-	0.1723	-
40	0.5397	1.25	0.0754	1.13	1.0867	0.82	0.0930	0.89
80	0.2418	1.16	0.0361	1.06	0.5103	1.09	0.0736	0.34
160	0.1133	1.09	0.0172	1.07	0.2507	1.02	0.0290	1.34
320	0.0567	1.00	0.0088	0.97	0.1263	0.99	0.0153	0.93
640	0.0283	1.00	0.0044	0.99	0.0629	1.00	0.0061	1.32
1280	0.0141	1.01	0.0022	1.01	0.0313	1.01	0.0029	1.07

TABLE 4  
*Errors and orders for two-dimensional Burgers-type equation: second-order scheme.*

N	Time = $0.5/(\pi^2)$				Time = $1.5/(\pi^2)$			
	$L^1$		$L^\infty$		$L^1$		$L^\infty$	
	Error	Order	Error	Order	Error	Order	Error	Order
20	0.35889	-	0.06713	-	0.54414	-	0.11403	-
40	0.09464	1.90	0.01852	1.86	0.18828	1.53	0.05742	0.99
80	0.02392	1.98	0.01166	0.67	0.04732	1.99	0.02200	1.38
160	0.00591	2.02	0.00468	1.32	0.01090	2.12	0.00990	1.29
320	0.00158	1.91	0.00196	1.25	0.00291	1.90	0.00512	0.81
640	0.00042	1.92	0.00081	1.28	0.00075	1.96	0.00323	0.67
1280	0.00011	1.95	0.00033	1.31	0.00019	1.96	0.00160	1.01

We recorded data at  $t_1 = 0.5/\pi^2$  (before singularity) and  $t_2 = 1.5/\pi^2$  (after singularity).

Errors and orders as measured in both  $L^1$ - and  $L^\infty$ -norms, before and after the singularity, are listed in Table 3. In Table 4, we list the  $L^1$ - and  $L^\infty$ -errors and orders for the numerical solutions by the second-order scheme, Algorithm 4. Resolution results are shown in Figure 4.2.

The results quoted in Table 3 show both  $L^1$ - and  $L^\infty$ -convergence rates of order  $\mathcal{O}(\Delta x)$  for both before and after the formation of singularity. The discrepancy between the optimal  $L^\infty$ -result of order  $\mathcal{O}(\sqrt{\Delta x})$  [CrLi84, So] and the result of Table 3 is explained in Example 1: Since all we can compute are solutions with finitely many singularities, one can not distinguish between the convergence rates of first-order H-J solutions when measured either by  $L^1$ - or  $L^\infty$ -norm—they both are of order  $\mathcal{O}(\Delta x)$ .

Table 4 quotes the results for the second-order central scheme, Algorithm 4. Here the  $L^1$ -measure of the error achieves the expected convergence rate of order  $\mathcal{O}(\Delta x)^2$ , in contrast to a lower rate of order  $\mathcal{O}(\Delta x)$  when measured in the  $L^\infty$ -norm.

Our numerical evidence supports the  $L^1$ -error estimates for the approximate solutions of *convex* multidimensional H-J equations by the authors, [LinTa]: The  $L^1$ -norm is more appropriate than the  $L^\infty$ -norm for convergence rate problems of H-J equations.

**4.2. High-resolution.** *Example 3* (one-dimensional). We solve a one-dimensional Riemann problem with a nonconvex Hamiltonian:

$$(4.3) \quad \begin{cases} \varphi_t + \frac{1}{4}(\varphi_x^2 - 1)(\varphi_x^2 - 4) = 0, \\ \varphi(x, 0) = -2|x|, \end{cases} \quad -1 \leq x \leq 1.$$

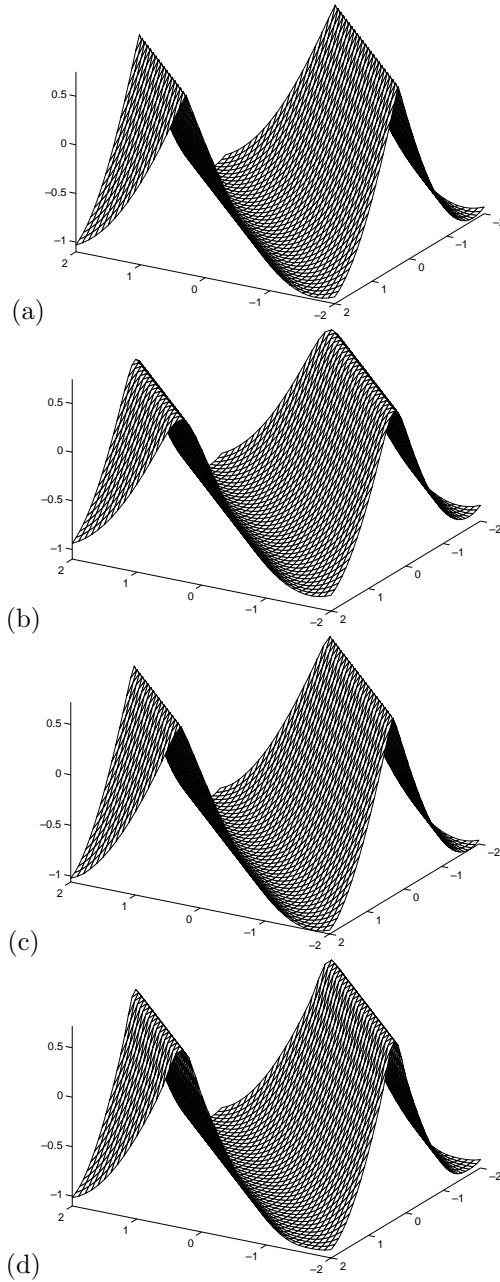


FIG. 4.2. After the singularity, at  $t = 1.5/\pi^2$ , Mesh:  $40 \times 40$ . (a) exact solution; (b)  $LxF$ ; (c) Min-Godunov; (d) second-order central scheme.

Numerical simulation at  $t = 1.0$  by the second-order scheme, Algorithm 2, is presented in Figure 4.3. We found that our numerical solutions converge toward the viscosity solution when the spatial step  $\Delta x$  becomes smaller. Without nonlinear limiters, numerical solutions may fail to converge to the viscosity solution; consult [HuSh] for details.

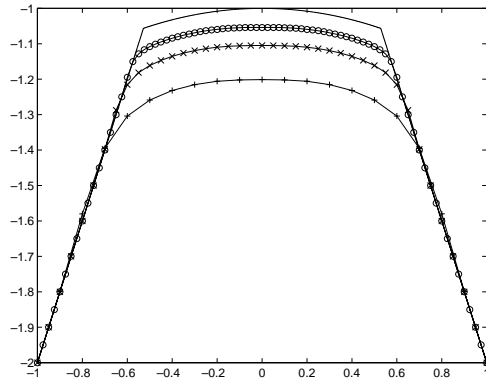


FIG. 4.3. Resolution for Example 3 via Algorithm 4, second-order. +: 20 points; x: 40 points; o: 80 points.

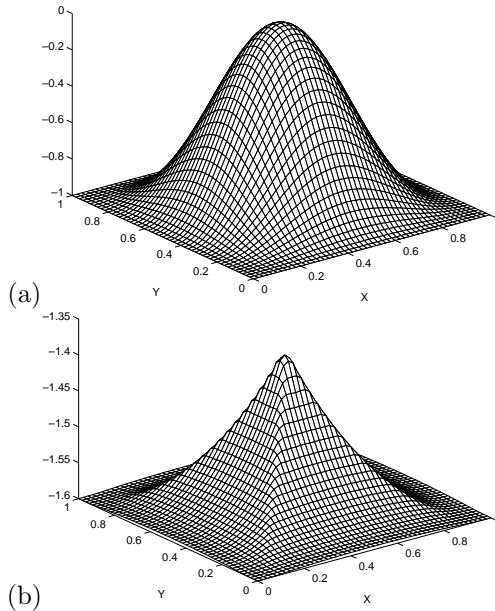


FIG. 4.4. Resolution of  $\varphi$  for Example 4 via Algorithm 4, second-order; Mesh:  $50 \times 50$ . (a) at  $t = 0$ ; (b) at  $t = 0.6$ .

*Example 4* (two dimensions). We solve another Cauchy problem for a two-dimensional H-J equation with a nonconvex Hamiltonian and a periodic boundary condition [OsSe, JiXi]:

$$(4.4) \quad \begin{cases} \varphi_t + \sqrt{\varphi_x^2 + \varphi_y^2 + 1} = 0, \\ \varphi(x, y, 0) = 0.25(\cos(2\pi x) - 1)(\cos(2\pi y) - 1) - 1, \end{cases} \quad 0 \leq x, y \leq 1.$$

Using the second-order scheme, Algorithm 4, we record data at  $t = 0.6$  (after singularity) with mesh  $50 \times 50$ . The graph of the numerical solution is presented in Figure 4.4. The *kink* singularity has been carefully studied in [JiXi].

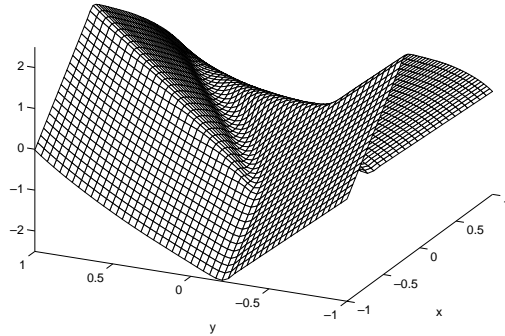


FIG. 4.5. Resolution at  $t = 1.0$  for Example 5 via Algorithm 4, second-order; mesh:  $50 \times 50$ .

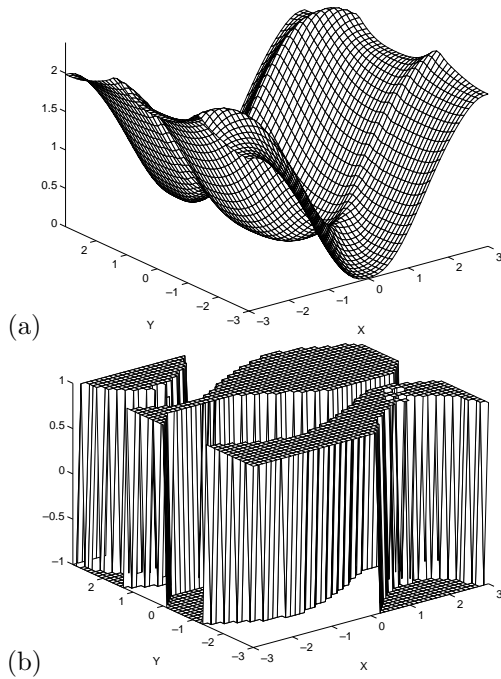


FIG. 4.6. Resolution at  $t = 1.0$  for Example 6 via Algorithm 5, second-order; mesh:  $50 \times 50$  (a) for  $\varphi$ ; (b) for  $\text{sign}(\varphi_y)$ .

*Example 5* (two dimensions). We solve a two-dimensional nonconvex Riemann problem with fixed boundary condition [OsSh]:

$$(4.5) \quad \begin{cases} \varphi_t + \sin(\varphi_x + \varphi_y) = 0, & -1 \leq x, y \leq 1. \\ \varphi(x, y, 0) = \pi(|y| - |x|), \end{cases}$$

We compute up to  $t = 1.0$  with mesh  $50 \times 50$ . The numerical resolution is presented in Figure 4.5.

*Example 6* (variable two dimensions). We solve the following problems related to control optimal cost determination [OsSh, JiPe]:

$$(4.6) \quad \begin{cases} \varphi_t - \sin(y)\varphi_x + \sin(x)\varphi_y + |\varphi_y| - \frac{1}{2} \sin(y)^2 - 1 + \cos(x) = 0, \\ \varphi(x, y, 0) = 0, \end{cases}$$

$-\pi \leq x, y \leq \pi$  with a periodic boundary condition.

The Hamiltonian depends on not only  $\nabla\varphi$  but also  $(x, y)$ . In this problem, the most interesting quantity is the optimal solution  $sign(\varphi_y)$ , discontinuities-in-derivative resolution [OsSh]. Numerical simulation by the second-order scheme, Algorithm 5, at  $t = 1.0$  with mesh  $50 \times 50$  is presented in Figure 4.6.

**5. Appendix: Construction of nearby approximations.** Here, we construct a nearby approximate solution like the one described in Theorem 3.1. We start with one-dimensional case.

Given grid-value  $\varphi_j$ , we define the new half-integer grid-value  $u_{j+\frac{1}{2}} := \frac{\Delta\varphi_j}{\Delta x}$ . (Compare with conservation laws in [CoFaNa].) Based on these values, we reconstruct a piecewise linear interpolant

$$u(x) = \sum_{j=-\infty}^{\infty} \left[ u_{j+\frac{1}{2}} + \frac{u'_{j+\frac{1}{2}}}{\Delta x} (x - x_{j+\frac{1}{2}}) \right] \chi_{I_{j+\frac{1}{2}}}.$$

Here  $\chi_{I_{j+\frac{1}{2}}}$  is the characteristic function over the interval  $I_{j+\frac{1}{2}} = [x_j, x_{j+1}]$  and the numerical derivative  $u'_{j+\frac{1}{2}}$  is computed in terms of the Max-Mod limiter [BrOs], i.e.,

$$u'_{j+\frac{1}{2}} = \max\{\Delta u_{j+\frac{1}{2}}, \Delta u_{j-\frac{1}{2}}\}.$$

To obtain the quadratic interpolant, we integrate the above piecewise linear interpolant,  $u(x)$ , from the far field, resulting in

$$\begin{aligned} \psi(x) &:= \int_{-\infty}^x u(y) dy \\ &= \varphi_n + u_{n+\frac{1}{2}}(x - x_n) + \frac{u'_{n+\frac{1}{2}}}{2\Delta x}(x - x_n)(x - x_{n+1}), \end{aligned}$$

where  $x$  lies in  $(x_n, x_{n+1})$ . We note that  $\psi(x_n) = \varphi_n$  for all integer grid points,  $x_n$ . Since  $\psi(x_n)$  is (one-side) differentiable, the semiconcave stability property may be checked by computing the difference of the left-hand side and right-hand side derivatives at each integer grid point. Thanks to the Max-Mod limiter, the difference is always nonnegative, which implies the semiconcave stability.

We now turn to the multidimensional case. For simplicity, we demonstrate our construction on the NW/SE mesh. We first demonstrate our construction of a nearby approximation over a triangle, say  $C_{j,k}^{NW}$  with vertices  $(x_j, y_k), (x_j, y_{k+1})$ , and  $(x_{j+1}, y_{k+1})$ . Following the one-dimensional construction and the consistency with the grid-values at the vertices, we obtain, on the triangle  $C_{j,k}^{NW}$ ,

$$\begin{aligned} &\psi_{j,k}^{NW}(x, y) \\ &= \varphi_{j,k} + \varphi'_{j+\frac{1}{2},k+1}(x - x_j) + \frac{\varphi''_{j+\frac{1}{2},k+1}}{2\Delta x}(x - x_j)(x - x_{j+1}) \\ &\quad + \varphi'_{j,k+\frac{1}{2}}(y - y_k) + \frac{\varphi''_{j,k+\frac{1}{2}}}{2\Delta y}(y - y_k)(y - y_{k+1}) \\ &\quad + \left( \frac{\sqrt{\Delta x^2 + \Delta y^2}}{2\Delta x \Delta y} \tilde{\varphi}_{j+\frac{1}{2},k+\frac{1}{2}} - \frac{1}{2\Delta y} \varphi''_{j+\frac{1}{2},k+1} - \frac{1}{2\Delta x} \varphi''_{j,k+\frac{1}{2}} \right) (x - x_j)(y - y_{k+1}). \end{aligned}$$

Here

$$\varphi'_{j+\frac{1}{2},k} = \frac{\Delta_x \varphi_{j,k}}{\Delta x}; \quad \varphi'_{j,k+\frac{1}{2}} = \frac{\Delta_y \varphi_{j,k}}{\Delta y}; \quad \tilde{\varphi}_{j+\frac{1}{2},k+\frac{1}{2}} = \frac{\varphi_{j+1,k+1} - \varphi_{j,k}}{\sqrt{\Delta x^2 + \Delta y^2}};$$

$$\varphi''_{j+\frac{1}{2},k} = \max \{ \Delta_x \varphi'_{j+\frac{1}{2},k}, \Delta_x \varphi'_{j-\frac{1}{2},k} \}; \quad \varphi''_{j,k+\frac{1}{2}} = \max \{ \Delta_y \varphi'_{j,k+\frac{1}{2}}, \Delta_y \varphi'_{j,k-\frac{1}{2}} \};$$

and

$$\tilde{\tilde{\varphi}}_{j+\frac{1}{2},k+\frac{1}{2}} = \max \{ \tilde{\varphi}_{j,k}, \tilde{\varphi}_{j-1,k-1} \}.$$

Similarly, the formula for the triangle  $C_{j,k}^{SE}$  with vertices  $(x_j, y_k), (x_{j+1}, y_k)$ , and  $(x_{j+1}, y_{k+1})$  is

$$\begin{aligned} & \psi_{j,k}^{SE}(x, y) \\ &= \varphi_{j,k} + \varphi'_{j+\frac{1}{2},k}(x - x_j) + \frac{\varphi''_{j+\frac{1}{2},k}}{2\Delta x}(x - x_j)(x - x_{j+1}) \\ & \quad + \varphi'_{j+1,k+\frac{1}{2}}(y - y_k) + \frac{\varphi''_{j+1,k+\frac{1}{2}}}{2\Delta y}(y - y_k)(y - y_{k+1}) \\ & \quad + \left( \frac{\sqrt{\Delta x^2 + \Delta y^2}}{2\Delta x \Delta y} \tilde{\tilde{\varphi}}_{j+\frac{1}{2},k+\frac{1}{2}} - \frac{1}{2\Delta y} \varphi''_{j+\frac{1}{2},k} - \frac{1}{2\Delta x} \varphi''_{j+1,k+\frac{1}{2}} \right) (x - x_{j+1})(y - y_k). \end{aligned}$$

Our nearby approximation can then be written as

$$\psi(x, y) = \sum_{j,k} \left( \psi_{j,k}^{NW}(x, y) \chi_{T_{j,k}^u} + \psi_{j,k}^{SE}(x, y) \chi_{T_{j,k}^l} \right).$$

To prove the semiconcave stability, we proceed as in the one-dimensional case: We compute the difference of the one-side directional derivatives between  $\psi_{j,k}^{NW}$  and  $\psi_{j,k}^{SE}$ . We note that the directional derivatives of  $\psi_{j,k}^{NW}$  (or  $\psi_{j,k}^{SE}$ ) at each integer grid point,  $(x_j, y_k)$ , can be decomposed as a *positive* linear combination of the directional derivatives of  $\psi_{j,k}^{NW}$  (or  $\psi_{j,k}^{SE}$ ) along the three main directions  $(0, 1)$ ,  $(1, 0)$ , and  $(1, 1)$ . Since our nearby approximations satisfy the semiconcave stability along these three main directions—thanks to the Max-Mod limiter, we conclude the semiconcave stability of  $\psi$  in any direction.

REFERENCES

[Ab] R. ABGRALL, *Numerical discretization of first-order Hamilton–Jacobi equation on triangular meshes*, Comm. Pure. Appl. Math., 49 (1996), pp. 1339–1373.

[BaCr] M. BARDI, M. CRANDALL, L. EVANS, H. SONER, AND P. SOUGANIDIS, *Viscosity Solutions and Applications*, in Lectures given at the second C.I.M.E., Motecatini Terme, Italy, I. Capuzzo Dolcetta and P.-L. Lions, eds., Lecture Notes in Math. 1660, Springer-Verlag, Berlin, 1997.

[Ba] G. BARLES, *Solution de Viscosité des Équations de Hamilton–Jacobi*, Springer-Verlag, Berlin, 1994.

[BrOs] Y. BRENIER AND S. OSHER, *The discrete one-sided Lipschitz condition for convex scalar conservation laws*, SIAM J. Numer. Anal., 25 (1988), pp. 8–23.

[CoFaNa] L. CORRIAS, M. FALCONE, AND R. NATALINI, *Numerical schemes for conservation laws via Hamilton–Jacobi equations*, Math. Comp., 64 (1995), pp. 555–580.

- [CrEvLi] M. G. CRANDALL, L. C. EVANS, AND P.-L. LIONS, *Some properties of viscosity solutions of Hamilton–Jacobi equations*, Trans. Amer. Math. Soc., 282 (1984), pp. 487–502.
- [CrLi83] M. G. CRANDALL AND P.-L. LIONS, *Viscosity solutions of Hamilton–Jacobi equations*, Trans. Amer. Math. Soc., 277 (1983), pp. 1–42.
- [CrLi84] M. G. CRANDALL AND P.-L. LIONS, *Two approximations of solutions of Hamilton–Jacobi equations*, Math. Comp., 43 (1984), pp. 1–19.
- [HaOs] A. HARTEN AND S. OSHER, *Uniformly high-order accurate nonoscillatory schemes. I*, SIAM J. Numer. Anal., 24 (1987), pp. 229–309.
- [HuSh] C. HU AND C.-W. SHU, *A discontinuous Galerkin finite element method for Hamilton–Jacobi equations*, SIAM J. Sci. Comput., 21 (1999), pp. 666–690.
- [JLLoT] G.-S. JIANG, D. LEVY, C.-T. LIN, S. OSHER, AND E. TADMOR, *High-resolution nonoscillatory central schemes with nonstaggered grids for hyperbolic conservation laws*, SIAM J. Numer. Anal., 35 (1998), pp. 2147–2168.
- [JiPe] G.-S. JIANG AND D. PENG, *Weighted ENO Schemes for Hamilton–Jacobi Equations*, UCLA CAM report 97-29, 1997.
- [JiTa] G.-S. JIANG AND E. TADMOR, *Nonoscillatory central schemes for multidimensional hyperbolic conservation laws*, SIAM J. Sci. Comput., 19 (1998), pp. 1892–1917.
- [JiXi] S. JIN AND Z. XIN, *Numerical passage from systems of conservation laws to Hamilton–Jacobi equations and relation schemes*, SIAM J. Numer. Anal., 35 (1998), pp. 2385–2404.
- [KoMaSo] G. KOSSIORIS, CH. MAKRIDAKIS, AND P. E. SOUGANIDIS, *Finite volume schemes for the Hamilton–Jacobi equations*, Numer. Math., 83 (1999), pp. 427–442.
- [Kr] S. N. KRUKOV, *The Cauchy problem in the large for nonlinear equations and for certain quasilinear systems of the first order with several variables*, Soviet Math. Dokl., 5 (1964), pp. 493–496.
- [KuTa] A. KURGANOV AND E. TADMOR, *New high resolution semi discrete central schemes for Hamilton–Jacobi equations*, J. Comput. Phys., to appear.
- [Le] O. LEPSKY, *Spectral Viscosity Approximations to Hamilton–Jacobi Solutions*, preprint.
- [LinTa] C.-T. LIN AND E. TADMOR,  *$L^1$ -stability and error estimates for approximate Hamilton–Jacobi solutions*, Numer. Math., to appear.
- [Li] P.-L. LIONS, *Generalized Solutions of Hamilton–Jacobi Equations*, Pitman, London, 1982.
- [LiSo] P.-L. LIONS AND P. E. SOUGANIDIS, *Convergence of MUSCL and filtered schemes for scalar conservation laws and Hamilton–Jacobi equations*, Numer. Math., 69 (1995), pp. 441–470.
- [LiuTa] X.-D. LIU AND E. TADMOR, *Third order nonoscillatory central scheme for hyperbolic conservation laws*, Numer. Math., 79 (1998), pp. 397–425.
- [NeTa90] H. NESSYAHU AND E. TADMOR, *Non-oscillatory central differencing for hyperbolic conservation laws*, J. Comput. Phys., 87 (1990), pp. 408–463.
- [NeTa92] H. NESSYAHU AND E. TADMOR, *The convergence rate of approximate solutions for nonlinear scalar conservation laws*, SIAM J. Numer. Anal., 29 (1992), pp. 1505–1519.
- [NeTaTa] H. NESSYAHU, E. TADMOR, AND T. TASSA, *The convergence rate of Godunov type schemes*, SIAM J. Numer. Anal., 31 (1994), pp. 1–16.
- [OsSe] S. OSHER AND J. SETHIAN, *Fronts propagating with curvature dependent speed: Algorithms based on Hamilton–Jacobi formulations*, J. Comput. Phys., 79 (1988), pp. 12–49.
- [OsSh] S. OSHER AND C.-W. SHU, *High-order essentially nonoscillatory schemes for Hamilton–Jacobi equations*, SIAM J. Numer. Anal., 28 (1991), pp. 907–922.
- [So] P. E. SOUGANIDIS, *Approximation schemes for viscosity solutions of Hamilton–Jacobi equations*, J. Differential Equations, 59 (1985), pp. 1–43.
- [Ta] E. TADMOR, *Local error estimates for discontinuous solutions of nonlinear hyperbolic equations*, SIAM J. Numer. Anal., 28 (1991), pp. 891–906.
- [TaTa] E. TADMOR AND T. TANG, *Pointwise error estimates for scalar conservation laws with piecewise smooth solutions*, SIAM J. Numer. Anal., 36 (1999), pp. 1739–1756.
- [TaTe] T. TANG AND Z.-H. TENG, *The sharpness of Kuznetsov’s  $O(\sqrt{\Delta x})$   $L^1$ -error estimate for monotone difference schemes*, Math. Comp., 64 (1995), pp. 581–589.